

# A New *Carodnia* Simpson, 1935 (Mammalia, Xenungulata) from the Early Eocene of Northwestern Peru and a Phylogeny of Xenungulates at Species Level

Pierre-Olivier Antoine · Guillaume Billet ·  
Rodolfo Salas-Gismondi · Julia Tejada Lara ·  
Patrice Baby · Stéphane Brusset · Nicolas Espurt

© Springer Science+Business Media New York 2014

**Abstract** In spite of a scarce fossil record and poor diversity, xenungulates cover a wide spatial range throughout South America: a new representative of *Carodnia* Simpson, 1935, attests to the northernmost occurrence of a carodniid xenungulate, ~4,500 km away from previous occurrences (Saõ José de Itaboraí, Rio de Janeiro, Brazil; Chubut Province, Patagonia, Argentina) and very close to the Pacific Coast. A phylogenetic analysis of Xenungulata at the species level shows that Xenungulata and Carodniidae are monophyletic, while Etayoidae are potentially paraphyletic, at least with the selected taxonomic sample. Phylogenetic relationships among Xenungulata are [*Notoetayoa gargantuai*, *Etayoabacatensis* [Carodnia sp. nov. [Carodnia feruglio, C. cf. feruglio, C. vieirai]]]. The new species is well differentiated from other xenungulates in having the m3 slightly smaller than m2 in terms of occlusal area and the entoconid

and hypoconid almost at the same level on m3. It further differs from all other xenungulates but *Etayoabacatensis* in possessing a transverse protolophid on m3. It is distinct from all other representatives of *Carodnia* in showing a precingulid strongly developed on m2-m3. Referral of the locality to the well-constrained early Eocene Mogollón Formation also confirms (i) the persistence of both carodniid and etayoid xenungulates well after the Paleocene-Eocene transition in South America and (ii) the absence of paleogeographic barrier for such large terrestrial mammals at the scale of South American landmass.

**Keywords** Chacra-Salina group · Mogollón formation · Phylogenetic analysis · Paleogeography · South American ungulates · Itaboraian-Riochican South American Land Mammal ages

**Electronic supplementary material** The online version of this article (doi:10.1007/s10914-014-9278-1) contains supplementary material, which is available to authorized users.

P.-O. Antoine (✉) · R. Salas-Gismondi  
Institut des Sciences de l'Évolution, CC064, Université Montpellier 2-CNRS-IRD, Place Eugène Bataillon, F-34095 Montpellier, France  
e-mail: pierre-olivier.antoine@univ-montp2.fr

G. Billet  
Centre de Recherche sur la Paléobiodiversité et les Paléoenvironnements, CR2P - UMR 7207 CNRS, MNHN, Univ Paris 06 - Muséum national d'Histoire naturelle, 8 rue Buffon, CP 38 75005 Paris, France

R. Salas-Gismondi · J. T. Lara  
Departamento de Paleontología de Vertebrados, Museo de Historia Natural-Universidad Nacional Mayor San Marcos, Avenida Arenales, 1256 Lima 11, Peru

J. T. Lara  
Florida Museum of Natural History - University of Florida, PO BOX 117800, Gainesville, FL 32611, USA

J. T. Lara  
Institut Français d'Etudes Andines, UMIFRE 17 MAEDI/CNRS  
USR 3337, Lima, Peru

P. Baby · S. Brusset  
Géosciences-Environnement Toulouse, Université de Toulouse; UPS (SVT-OMP); LMTG; CNRS; IRD, 14 Avenue Édouard Belin, F-31400 Toulouse, France

P. Baby · S. Brusset · N. Espurt  
Convenio IRD-PeruPetro, Av. Luis Aldana 320, San Borja, Lima, Peru

N. Espurt  
CEREGE, CNRS, IRD, UM34, Technopôle Environnement Arbois-Méditerranée, Aix-Marseille Université, BP80, F-13545 Aix-en-Provence Cedex 04 Marseille, France

## Introduction

Xenungulata are probably the most enigmatic order of South American ungulates, with a fossil record thus far restricted to the early Paleocene-early Eocene interval in Patagonia, Brazil, and Colombia (Simpson 1935; Paula Couto 1952; Villarroel 1987; Gelfo et al. 2008; Clyde et al. 2014; Woodburne et al. 2014a, b). Their known alpha-diversity is very low, with only four species included within three genera. Two families are formally recognized within Xenungulata: (1) the monotypic Carodniidae Paula Couto, 1952, with *Carodnia feruglio* Simpson, 1935 (late early Paleocene, Patagonia) and *Carodnia vieirai* Paula Couto, 1952 (early Eocene, Brazil), and (2) the Etayoidae Villarroel 1987, with *Etayoaa bacatensis* Villarroel, 1987 (earliest Eocene, Colombia; Bayona et al. 2010; Morón et al. 2013) and *Notoetayoaa gargantua* Gelfo, López, and Bond, (late early Paleocene, Patagonia). Another xenungulate, so far undescribed and unnamed, was also mentioned in the Río Loro Formation of northwestern Argentina (Fig. 1b; Bergqvist et al. 2004), probably early Eocene in age (Aguas Chiquitas, Itaboraian South American Land Mammal Age [SALMA]; Woodburne et al. 2014a, b).

Xenungulates include the largest South American mammals in early Paleogene times, with body mass estimates for *Carodnia vieirai* reaching ~450 kg up to 720 kg, based on the area of m1 (specimen DGM-334, stored in the Divisaõ de Geologia e Mineralogia do Departamento Nacional da Produçaõ mineral, Brazil; “ungulates” regression equation of Legendre 1989) or on the m1-m3 length on DGM-334 (“non-selenodont ungulates” regression equation; Damuth 1990), respectively. Supraordinal affinities of these buno-lophodont graviportal herbivores are disputed and they have rarely been investigated phylogenetically (e.g., Cifelli 1993; Bergqvist 1996; O’Leary et al. 2013). Concerning the investigations of intraordinal relationships, only one formal phylogeny including a comprehensive sample of xenungulates has been published to date (Gelfo et al. 2008).

The current article aims at describing a new specimen of xenungulate found by one of us (NE) in February 2012, in the Talara Basin, northwesternmost Peru, and excavated in April 2012 (by RSG, JTL, and PB). The locality is situated at midway between the cities of Talara and Tumbes and about 20 km away from the Pacific Coast (Fig. 1a). More precisely, the mandibular fragment MUSM-2025 was found in the Quebrada Cabeza de Vaca, ~5 km upstream its junction with the Quebrada Seca. The corresponding deposits are coarse-grained fluvial sandstones of the Upper Mogollón Member, topping the Mogollón Formation (sensu Fildani et al. 2008: Fig. 4). This formation is referred to the lower part of the early Eocene Chacra-Salina Group, composed of marine to continental-derived sandstones and conglomerates (e.g., Iddings and Olsson 1928; Séranne 1987; Higley 2004). The Mogollón Formation is entirely Ypresian in age, based on

nanno-, micro-, and macrofossil biochronology (nannoplankton, palynomorphs, foraminifers, and macroinvertebrates; Petters 1968; Fildani 2004; Fildani et al. 2008). Moreover, the Upper Mogollón Member is the only ante-Oligocene stratigraphic unit of fluvial origin recorded in the Talara Basin (Fildani et al. 2008).

## Material and Methods

In the field, the specimen MUSM-2025 was found within a coarse-grained sandstone block, broken into lingual and labial halves. The fitting parts were glued together during the restoration process. The dental nomenclature as discussed and defined by Gelfo et al. (2008) will be used throughout the text.

The phylogenetic analysis is based on a deeply reworked version of Gelfo et al.’s (2008) taxa-character matrix, focused on dental and mandibular characters known for the new specimen and most other xenungulates (Appendices 1 and 2). The phylogenetic rationale, notably for scoring multistate and polymorphic characters, is adapted from that of Antoine (2002). The most parsimonious trees and the strict consensus tree were obtained using PAUP 4.0 V.10 (Swofford 1998), based on 34 morphological characters scored in nine terminal taxa, including an exhaustive sample for Xenungulata at the species level, with *Alcidedorbignya inopinata* Muizon and Marshall, 1987, *Asmithwoodwardi scotti* Paula Couto, 1952, and *Didolodus multicuspis* Ameghino, 1897, as outgroups. Branch support was assessed using Bremer indices (Bremer 1994). See **Electronic Supplementary Material** for further details.

**Institutional Abbreviations** AMNH, American Museum of Natural History, New York, USA; DGM, Divisaõ de Geologia e Mineralogia do Departamento Nacional da Produçaõ mineral, Brazil; GM, Departamento de Geociencias, Universidad Nacional de Colombia, Bogotá, Colombia; MHNC, Museo de Historia Natural de Cochabamba, Bolivia; MNHN, Muséum National d’Histoire Naturelle, Paris; MPEF, Museo de Paleontología Egidio Feruglio, Trelew, Argentina; MUSM, Museo de Historia Natural de la Universidad Nacional Mayor San Marcos, Lima, Peru; UM2, Université Montpellier 2, France.

## Systematic Paleontology

Order XENUNGULATA Paula Couto, 1952  
 Family CARODNIIDAE Paula Couto, 1952  
 Genus *Carodnia* Simpson, 1935



**Fig. 1** **a** Simplified geological map of northwesternmost Peru. The early Eocene xenungulate *Carodnia inexpectans* sp. nov. was found in the Quebrada Cabeza de Vaca, between Talara and Tumbes, as indicated by the red star (black star in printed version). **b** Map detailing the

documented occurrences of Xenungulata (Carodniidae and Etayoidea) in South America. Based on data from Simpson (1935), Paula Couto (1952), Villarroel (1987), Gelfo et al. (2008), Clyde et al. (2014), Woodburne et al. (2014a, b), and the present work

#### *Ctalecarodnia* Simpson, 1935

Type species: *Carodnia feruglio* Simpson, 1935

Stratigraphic range: Late early Paleocene-early Eocene (late Danian-Ypresian standard ages; “*Carodnia Zone*” and Itaboraian-Riochican SALMAs), sensu Gelfo et al. (2009), Clyde et al. (2014), and Woodburne et al. (2014a, 2014b).

Geographic range: South America (Argentinean Patagonia, eastern Brazil, and northwestern Peru).

Emended diagnosis: Large xenungulates with a mandibular foramen located above the dorsal edge of the dentary, a mandibular branch partly hiding m3 in lateral view, with a paracristid low and almost parallel to the protolophid, with

hypoconid, hypoconulid, and cristid obliqua being part of/not differentiated from the hypolophid on m<sub>2</sub>, and with a weak paracristid on m<sub>3</sub>, but without a paraconid on m<sub>2</sub>-m<sub>3</sub>.

*Referred species:* *Carodnia vieirai* Paula Couto, 1952; *Carodnia* cf. *C. feruglooi* (Gelfo et al. 2008); *C. inexpectans* sp. nov.

*Carodnia inexpectans* sp. nov.

(Fig. 2)

*Holotype and only specimen:* MUSM-2025, a fragmentary right dentary with m<sub>2</sub> and m<sub>3</sub> and the alveoli of m<sub>1</sub>.

*Etymology:* From Latin *inexpectans* =unexpected, in reference to the unexpected occurrence of a carodniid xenungulate in northwestern South America.

*Geographic provenance:* Quebrada Cabeza de Vaca, 5 km upstream its junction with the Quebrada Seca (4.107° S; 80.886° W), Talara Basin, Departamento de Tumbes, Peru.

*Stratigraphic provenance and age:* Upper Mogollón Member, Mogollón Formation, Chacra-Salina Group, early Eocene (Ypresian standard age, Itaboraian or Riochican SALMAS; Fildani et al. 2008; Woodburne et al. 2014a, 2014b).

*Diagnosis:* Medium-sized *Carodnia* differing from other xenungulates in having m<sub>3</sub> slightly smaller than m<sub>2</sub> in terms of occlusal area and the entoconid and hypoconid almost at the same level on m<sub>3</sub>. Further differs from all other xenungulates but *Etayoaa bacatensis* in possessing a protolophid transverse on m<sub>3</sub>. Distinct from all other representatives of *Carodnia* in showing a precingulid strongly developed on m<sub>2</sub>-m<sub>3</sub>. Differs from *C. vieirai* and *C. feruglooi* in having a hypoconulid as high as the protolophid, but no ectocingulid on the distal part of m<sub>3</sub>. Distinct from *C. vieirai* and *C. cf. feruglooi* in showing a faint ectocingulid on m<sub>3</sub>. Further differs from *C. vieirai* in having a high mandibular body and a preingular stylid on m<sub>2</sub>-m<sub>3</sub>.

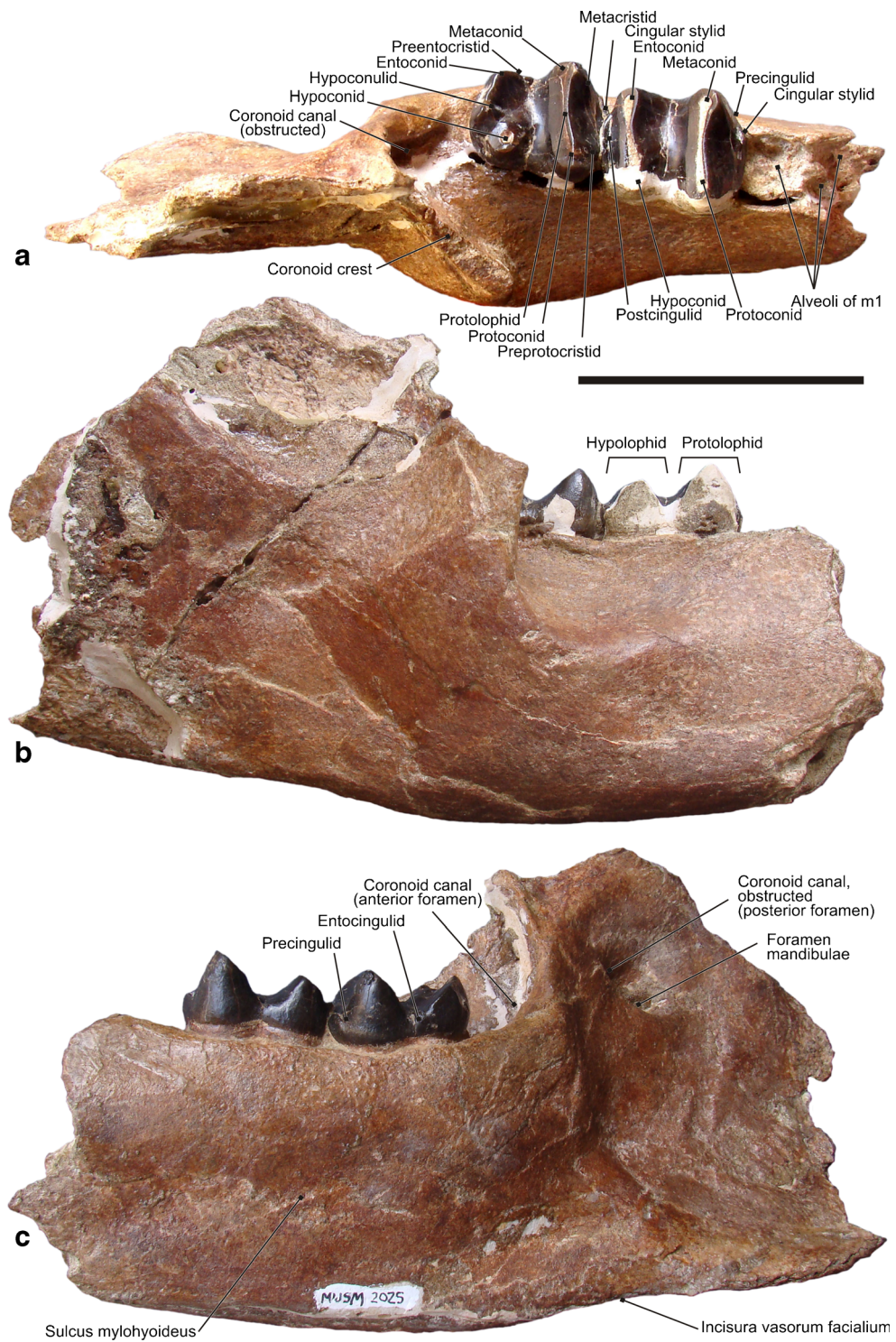
*Description and comparisons:* Mandible. The fragmentary right hemimandible MUSM-2025 preserves m<sub>2</sub> and m<sub>3</sub>, and both alveoli of a much smaller m<sub>1</sub>, as observed in all xenungulates (e.g., Paula Couto 1952; Villarroel 1987), the Oligocene pyrothere *Pyrotherium* Ameghino, 1888 (e.g., Shockey and Anaya 2004; Wilson et al. 2012), and the early Paleocene pantodont *Alcidedorbignya* (Muizon and Marshall 1992) (Fig. 2a). The region anterior to m<sub>1</sub> is broken away, as is the mandibular angle and most of the mandibular branch. The mandibular body is robust, with a convex ventral profile below m<sub>2</sub>-3 in lateral view, as in *Carodnia vieirai*, *Etayoaa bacatensis*, and *Alcidedorbignya* (Muizon and Marshall 1992). With respect to the length of m<sub>2</sub>+m<sub>3</sub>, the height of the body (Fig. 2b) is at the same time higher than that of *Notoetayoaa gargantuai* (Gelfo et al. 2008) and much lower than those of *C. vieirai* (e.g., twice as low as DGM-333; Paula Couto 1952) and *Etayoaa bacatensis* (Villarroel 1987). The coronoid crest that marks the anterior edge of the insertion for the M. masseter medialis is salient, forming an oblique ridge

pointing anteroventrally on the dorsal half of the lateral side of the body, as in the holotype of *C. vieirai* (DGM-333; Paula Couto 1952) and in *E. bacatensis*. The corresponding region is broken in DGM-334 (*C. vieirai*) and *N. gargantuai*, and unknown in *C. feruglooi*. The ventral edge shows a shallow facial vein notch (Fig. 2c) comparable to what is observed in the holotype of *C. vieirai*. However, it is much shallower in the latter specimens than in DGM-334 (*C. vieirai*; Paula Couto 1952), and in *E. bacatensis* (Villarroel 1987). Accordingly, the lower part of the mandibular angle was not as ventrally situated as observed in DGM-334 (*C. vieirai*) and *E. bacatensis*, but similar to what occurs in DGM-333 (*C. vieirai*). There is no retromolar space, and the anterior border of the ascending ramus partly hides m<sub>3</sub> in lateral view, as in both available mandibles of *C. vieirai*. This is a major discrepancy between MUSM-2025 and *C. vieirai* on the one hand, and Etayoidae on the other hand: the retromolar space is developed and m<sub>3</sub> is entirely visible in labial view in both *E. bacatensis* (observed) and *N. gargantuai*. Nevertheless, the retromolar space is much shorter in the latter than in the former (based on direct observation of MNHN casts of GM-32 and MPEF-PV 1871).

The ascending mandibular ramus displays a deep, high, and narrow fissure on its rostral side (Fig. 2a and c), strongly reminiscent of the coronoid foramen of the coronoid canal (sensu Tassy and Shoshani 1988) as observed in *C. vieirai* (DGM-333 and DGM-334). A similar fissure is most likely present in *N. gargantuai* and in *E. bacatensis*, and is assumed to coincide with an obstructed coronoid canal. On the lingual side of the mandibular ramus, a deep fossa, 10mm-wide and open distodorsally, includes both a wide mandibular foramen (facing ventrally) and an obstructed horizontal canal, oriented rostrally toward the fissure mentioned above (Fig. 2c). The mandibular foramen is also located above the dorsal edge of the mandibular body and almost at the same level as the occlusal surface of the molars. The coronoid canal (through which passes a branch of the lingual nerve) is considered a synapomorphy of Proboscidea, Tethytheria, Paenungulata, or Afrotheria (Tassy and Shoshani 1988; Ferretti and Debruyne 2011; Tabuce et al. 2012); it is also variably present in several non-afrotherian mammals (lagomorphs, artiodactyls, perissodactyls, and xenarthrans, where it can be obstructed in adults; see Tabuce et al. 2012) and in some notoungulates (e.g., *Plesiotypotherium* Villarroel, 1974). The mylohyoid sulcus is well marked, forming a sagittal groove at mid-height of the mandibular body on its lingual side (Fig. 2c).

*Teeth.* Enamel is thick (up to 2mm on worn lophids). Vertical Hunter-Schreger bands are not visible, contrary to what is mentioned for *C. vieirai* (Line and Bergqvist 2005) and *C. cf. feruglooi* (Gelfo et al. 2008) (Fig. 2b). Dental dimensions of MUSM-2025 widely exceed those of etayoids but fall within the size range of *Carodnia* (Table 1; Fig. 3). More precisely, they are larger than those of *C. feruglooi*

**Fig. 2** *Carodnia inexpectans* sp. nov., fragmentary right dentary with m2-m3 (MUSM-2025, holotype and only specimen), Mogollón Formation, early Eocene, Quebrada Cabeza de Vaca, northwestern Peru. **a** Occlusal view and dental nomenclature (adapted from Gelfo et al. 2008). **b** Labial view. **c** Lingual view showing the coronoid canal and the mandibular foramen. Scale bar = 5 cm



(holotype, cast AMNH 27886; Simpson 1935) and of *C. cf. feruglio* (MPEF-PV 1872; Gelfo et al. 2008), and smaller than those of *C. vieirai* (two specimens; Paula Couto 1952). The width/length ratios of m2 and m3 (0.86 and 0.90, respectively) are a bit higher in MUSM-2025 (Fig. 3; Table 2) than in *Etayoia bacatensis* (0.79 and 0.82) and in *Notoetayoia gargantuai* (0.78 on m3), much higher than in *C. feruglio*

(0.72 on m3) and in *C. cf. feruglio* (0.69 and 0.75; probably narrower due to post-mortem deformation), but similar to what is observed in *C. vieirai* (0.85 and 0.84). Both carodniids (*Carodnia*) and etayoids (*Etayoia* + *Notoetayoia*) encompass specimens with a wide size range, at least from a dental perspective, but these size ranges are far from overlapping, and MUSM-2025 falls unambiguously within *Carodnia*

**Table 1** Compared measurements for the second and third lower molars of xenungulates, in mm. After Simpson (1935), Paula Couto (1952), Villarroel (1987), Gelfo et al. (2008), and original data based on casts housed in the MNHN and in the UM2. Estimated values are between brackets

Tooth	Taxon	Length	Trigonid width	Talonid width	Crown height	References
m2	<i>Carodnia inexpectans</i>	26.4	22.8	20.9	22.0	<i>This work</i>
	<i>Carodnia feruglioii</i>	—	—	—	—	Simpson 1935
	<i>Carodnia cf. feruglioii</i>	(22.3)	(15.4)	—	—	Gelfo et al. 2008
	<i>Carodnia vieirai</i>	28.8–34.5	27.2–29.2	—25.0	—21.5	Paula Couto 1952
	<i>Etayoaa bacatensis</i>	6.1	4.8	(4.5)	—	Villarroel 1987
m3	<i>Carodnia inexpectans</i>	25.1	22.6	20.1	13.0	<i>This work</i>
	<i>Carodnia feruglioii</i>	24.3	17.5	15.5	—	Simpson 1935
	<i>Carodnia cf. feruglioii</i>	24.8–25.8	18.6–19.2	17.1–17.7	—	Gelfo et al. 2008
	<i>Carodnia vieirai</i>	34.0–39.0	30.5–30.5	—26.7	—19.8	Paula Couto 1952
	<i>Etayoaa bacatensis</i>	7.8	6.4	(5.2)	—	Villarroel 1987
	<i>Notoetayoaa gargantuaai</i>	14.7	11.5	9.5	—	Gelfo et al. 2008

(Fig. 3). Despite the wide size range observed within Xenungulata, there is no allometric variation either for m2 or for m3 shape ratios, as linear regression lines are well

supported for both dental loci ( $y=0.9035x - 1.4804$ , with  $R^2=0.9502$  on m2;  $y=0.8763x - 1.321$ , with  $R^2=0.9653$  on M3; Fig. 3). Another peculiarity of *C. inexpectans* sp. nov. is

**Fig. 3** Comparison of dental width/length ratios for Xenungulata. **a** Second lower molar (m2). **b** Third lower molar (m3). Based on measurements from Simpson (1935), Paula Couto (1952), Villarroel (1987), Gelfo et al. (2008), Woodburne et al. (2014a, b), and personal observation

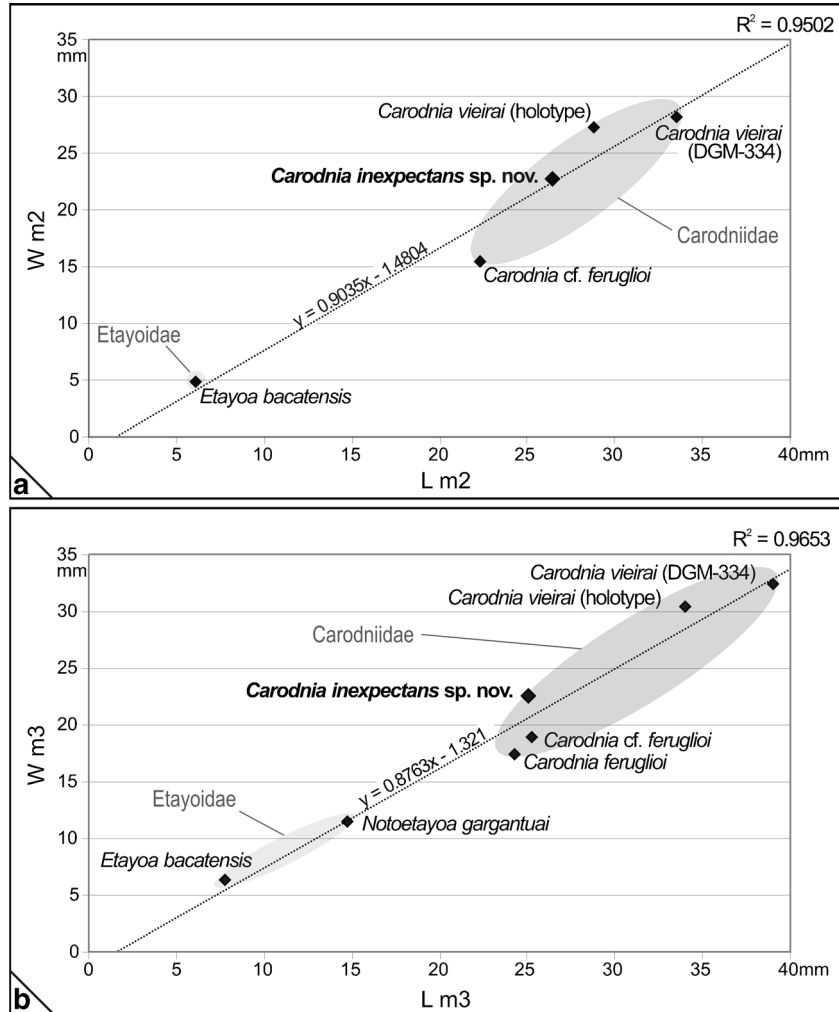


**Table 2** Comparison of width/length and area ratios for the second and third lower molars of xenungulates, in mm. Corresponding dimensions are detailed in Table 1

Taxon	W/L m2	W/L m3	L*W m3/L*W m2
<i>Carodnia inexpectans</i> sp. nov.	0.86	0.90	0.94
<i>Carodnia feruglio</i>	—	0.72	—
<i>Carodnia cf. feruglio</i>	0.69	0.75	1.24
<i>Carodnia vieirai</i>	0.85	0.84	1.32–1.34
<i>Etayoia bacatensis</i>	0.79	0.82	1.70
<i>Notoetayoia gargantuai</i>	—	0.78	—

the small size of m3 with respect to m2: the ( $W^*L\ m3 / W^*L\ m2$ ) ratio is lesser than 1 (0.94) in the Peruvian specimen, whereas this ratio ranges between 1.24 and 1.34 in other representatives of *Carodnia* and it attains 1.70 in *Etayoia bacatensis* (Table 2).

The molars are brachydont, in a way similar to what is observed in both *Carodnia* and Etayoidae (Simpson 1935; Paula Couto 1952; Villarroel 1987; Gelfo et al. 2008). As in all other known specimens referred to as *Carodnia*, the trigonid basin of m2 and m3 is delimited by a wide and strong protolophid, a low and smooth preprotocristid, and a faint premetacristid. Both cristids are pointing to the precingulid without connecting it (Fig. 2a and b). The precingulid is continuous and well developed all along the anterior side of both m2 and m3 (much more than in specimens referred to as *Carodnia*), with a salient stylid located at the lingual third of it (Fig. 2a). This stylid occurs in *Carodnia*, except in *C. vieirai*; its presence is variable in Etayoidae (only present on the m1 of *Etayoia* and the m3 of *Notoetayoia*; J. N. Gelfo, pers. comm. 2014). It is worn on both m2 and m3, and unveiling lozengic dentine pits on MUSM-2025, contrary to what is observed in other xenungulate specimens (where it is either unworn for a comparable gross dental wear, or absent). Like in *Carodnia*, but unlike in etayoids (Gelfo et al. 2008), there is no paraconid on m2 or m3 (Fig. 2a). Those stylids are not likely to be homologous with the latter cusp, as both a cingular stylid and a paraconid co-occur in *Etayoia* and *Notoetayoia* (Villarroel 1987; Gelfo et al. 2008). The protolophid of both m2 and m3 is thick and continuous, delimited by a transversely elongated flat wear facet oriented up- and backward at ~45° from the horizontal line. On m2, wear was sufficient to denude the dentine, whereas wear has not reached the enamel-dentine junction on the protolophid of m3. The second molar is fully bilophodont, with lophids at the same time parallel one to another and nearly transversely oriented, i.e., pointing less mesiolabially than in other xenungulate specimens except *E. bacatensis* (Villarroel 1987). The protolophid and hypolophid are almost equally developed in occlusal view

(Fig. 2a), even if the hypolophid is less elevated than the former in lateral view (Fig. 2b and c).

On m3, the talonid cusps are not significantly lower than the protolophid (Fig. 2c). In particular, the hypoconulid is elevated, notably with respect to the hypoconid and the entoconid, being as high as the protolophid in lingual view. The basin of the talonid is closed distally by the hypoconulid and the entoconid and open mesially. The hypoconid is thick and well differentiated on m3, as in all known specimens of *Carodnia* (Gelfo et al. 2008). There is a groove between the hypoconulid, high and unworn, and the well-developed hypoconid, delimited by a circular dentine pit and a dihedral wear facet. There is no postcristid running distally from the labial side of the entoconid on m3, contrary to what occurs in *C. vieirai* (DGM-334) and *C. cf. feruglio*. The distal root of m3 is pointing distoventrally, as in *N. gargantuai* (Gelfo et al. 2008). There is neither ento- nor ectocingulid on m2, similarly to what is observed in *E. bacatensis*, whereas a faint pad-like ectocingulid restricted to the talonid prolongs the postcingulid in *C. vieirai*. The mesial part of the entocingulid is faintly developed on m3, restricted to smoothly crenulated rugosities running on the mesiolingual side and fading away distally from the strong precingulid toward the base of the metaconid (Fig. 2c). The ectocingulid is similarly low, smooth, and weak, but probably more continuous (i.e., assumed to run from the level of the protoconid backward to that of the hypoconulid). There is no entocingulid between the entoconid and the hypoconulid, as in *E. bacatensis* (Villarroel 1987). Between the hypoconid and the hypoconulid, the ectocingulid is low, weak, and somewhat crenulated, as observed in *C. cf. feruglio* but far less developed than in *C. feruglio* and *C. vieirai* (DGM-334), where it surrounds the tooth from the protoconid back to the hypoconulid.

## Phylogenetic Relationships

The aims of this section are (i) to highlight phylogenetic relationships within Xenungulata, at the species/specimen level, (ii) to test the monophyly of both Etayoidae and Carodniidae (as supported and questioned by Gelfo et al. (2008), respectively), and (iii) to assess the phylogenetic affinities of *Carodnia inexpectans* sp. nov. within *Carodnia*. The character list appears in Appendix 1; further details are available as [Electronic Supplementary Material](#).

Nine terminal taxa were included in the phylogenetic analysis. The character coding sources (either direct observation and/or literature) are provided in Table 3. Three terminals were selected as outgroups: the early Paleocene pantodont *Alcidedorbignya inopinata* and the condylarths *Asmithwoodwardia scotti* (early Eocene), and *Didolodus*

**Table 3** Character coding sources (direct observation and/or literature) for each terminal taxon included within the present phylogenetic analysis. Taxa are arranged in alphabetical order (three outgroups first, then in-group taxa). See *Material and Methods* section for detail on institutional abbreviations

Terminal taxon	Character coding (source)	
	Direct observation	Literature
<i>Alcidedorbignya inopinata</i> Muizon and Marshall, 1987	MHNC specimens, currently deposited at MNHN	Muizon and Marshall 1987, 1992
<i>Asmithwoodwardia scotti</i> Paula Couto, 1952	—	Paula Couto 1952
<i>Didolodus multicuspis</i> Ameghino, 1897	MNHN cast of MACN 10689	Ameghino 1897; Gelfo et al. 2008; Gelfo 2010
<i>Carodnia feruglio</i> Simpson, 1935	AMNH	Simpson 1935
<i>Carodnia cf. feruglio</i>	—	Gelfo et al. 2008
<i>Carodnia inexpectans</i> sp. nov.	MUSM	<i>This work</i>
<i>Carodnia vieirai</i> Paula Couto, 1952	DGM; UM2 (cast)	Paula Couto 1952
<i>Etayo bacatensis</i> Villarroel, 1987	MNHN cast of GM-32	Villarroel 1987
<i>Notoetayo gargarua</i> Gelfo et al., 2008	MNHN cast of MPEF 1871	Gelfo et al. 2008

*multicuspis* (middle Eocene; see Gelfo 2010). Thirty-four morphological characters were scored (Appendices 1 and 2).

Six most parsimonious trees (49 steps; Consistency Index=0.8776; Retention Index=0.8605) were obtained by using the exhaustive search of PAUP 4.0 v.10 (Branch-and-Bound; unweighted parsimony; Swofford 1998). The same six most parsimonious trees (MPTs) were retained by using Hennig86 1.5 (Farris 1988), with similar lengths and indices. The strict consensus tree (length: 50 steps) is illustrated in Fig. 4.

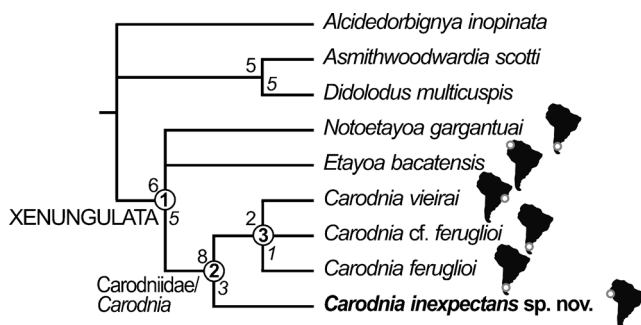


**Fig. 4** Phylogenetic relationships of *Carodnia inexpectans* sp. nov. within Xenungulata. Strict consensus tree of six most parsimonious trees (49 steps; CI=0.8776; RI=0.8605) obtained using PAUP 4.0 v.10 (Swofford 1998), based on 34 morphological characters, and performed on nine terminal taxa, including an exhaustive sample for Xenungulata at the species level, with *Alcidedorbignya inopinata*, *Asmithwoodwardia scotti*, and *Didolodus multicuspis* as outgroups. Suprageneric group names are based on current phylogenetic relationships and match those proposed by Villarroel (1987) and Gelfo et al. (2008). The number of unambiguous synapomorphies for each node appears above the internal branches left to the corresponding node. Branch support (bremer indices; Bremer 1994) is indicated for each node, and italicized. The nodes discussed in the text are designated by a circled number. See Electronic Supplementary Material for further details

Xenungulata and Carodniidae are monophyletic, while Etayoidae are potentially paraphyletic, with the selected taxonomic sample. Phylogenetic relationships among Xenungulata are [*Notoetayo gargarua*, *Etayo bacatensis* [*Carodnia inexpectans* sp. nov. [*Carodnia feruglio*, *C. cf. feruglio*, *C. vieirai*]]]]. Three distinct topologies are retained as regards Etayoidae among the MPTs ([*Notoetayo* [*Etayo*, *Carodnia*]]; [*Etayo* [*Notoetayo*, *Carodnia*]]; [*Carodnia* [*Notoetayo*, *Etayo*]])], which coincides with the first polytomy within the strict consensus tree (Fig. 4). In other words, albeit not supported unambiguously, the monophyly of Etayoidae cannot be ruled out. Two topologies are observed in MPTs within *Carodnia* (second polytomy; Fig. 4: [*C. cf. feruglio* [*C. feruglio*, *C. vieirai*]] and [*C. feruglio* [*C. cf. feruglio*, *C. vieirai*]]]). Accordingly, the specific assignment of *C. cf. feruglio* (sensu Gelfo et al. 2008) to a named species cannot be ascertained, while is discarded its referral to *C. feruglio* (a hypothesis not supported in MPTs), thus confirming most observations and conclusions of Gelfo et al. (2008).

The monophyly of Xenungulata is well supported by six unambiguous mandibular and dental synapomorphies, such as the presence of a coronoid canal likely to be obstructed (optimized in *C. feruglio* and *E. bacatensis*), of a high mandibular body, of a protolophid well developed, high and with a wear facet projected distally and well differentiated on the distal wall of the trigonid of m2-m3, of a very short and reduced cristid obliqua on m3, of an entoconid associated with the hypoconulid as a lophid that joins the postcristid and the entocristid on m3, of a distal root pointing distoventrally on m3, and of the absence of a precingular stylid on m2-m3 (see *Electronic Supplementary Material*). Although consisting of a single and fragmentary specimen (a partial dentary with m2, m3, and the alveoli of m1), the material here described

(MUSM-2025) is unambiguously referable to a representative of the large xenungulate *Carodnia*. *Carodnia* as a monophyletic genus including *C. inexpectans* sp. nov., *C. feruglio*, *C. vieirai*, and *C. cf. feruglio*, is supported by eight unambiguous mandibular and dental synapomorphies: mandibular foramen located above the dorsal edge of the dentary; mandibular ramus partly hiding m3 in lateral view; paraconid absent on m2-m3; trigonid of m2-m3 with a paralophid long, low, and almost parallel to the protolophid; hypoconid, hypoconulid, and cristid obliqua being part of/not differentiated from the hypolophid on m2; paracristid weak on m3.

Two unambiguous dental synapomorphies support the unresolved clade encompassing *C. feruglio*, *C. vieirai*, and *C. cf. feruglio* (precingulid weak on m2-m3; hypoconulid low on m3). Three other ambiguous synapomorphies are likely to further support its robustness (mandibular body very high; ectocingulid thick and continuous; ectocingulid reaching the talonid on m3) when more mandibular and/or dental material of *C. feruglio* or *C. cf. feruglio* is found. Aside from the two (up to five) synapomorphies discussed above, the specimen MUSM-2025 is well differentiated from other representatives of *Carodnia* in having three unambiguous autapomorphies (occlusal area of m3 smaller than that of m2; entoconid and hypoconid almost at the same level on m3; protolophid transverse on m3), thus supporting a distinct specific assignment among *Carodnia* (see systematic discussion in previous section). On the other hand, other representatives of *Carodnia* are not much differentiated one from another in terms of formal autapomorphies, with only one ambiguous reversal in *C. feruglio* (ectocingulid faint on m3) and in *C. cf. feruglio* (no ectocingulid on the talonid of m3), and one unambiguous reversal in *C. vieirai* (precingular stylid absent on m2-m3).

### Paleogeographic Implications

The current work attests to the first occurrence of a carodniid xenungulate in northern South America. Moreover, the attested occurrences of *Carodnia* are located c. 4,500 km from each other (Fig. 1b). Although very scarce, the xenungulate record almost covers the entire surface of South American emerged lands, of either Pacific or Atlantic affinities (Fig. 1b).

Paleogeographical data are concordant for the early Paleocene-early Eocene interval, with South America as a landmass isolated from Central and North America, but lacking any interior physical barrier (Lundberg et al. 1998; Hoorn et al. 2010; Roddaz et al. 2010;

Woodburne et al. 2014a). Yet, new data from the Madre de Dios Basin in southeastern Peru show the existence of a marine corridor – of unknown connection and spatio-temporal extent, though – in the Andean foreland during the late Paleocene (Outerbach et al. 2014) that may have promoted allopatric speciation within *Carodnia* and Etayoidea before Ypresian times (and the record of *C. vieirai*, *C. inexpectans* nov. sp., and *E. bacatensis*; Figs. 1b and 4). This record documents an interval very close to the Early Eocene Climatic Optimum (e.g., Zachos et al. 2008; Woodburne et al. 2014a, b). The early Eocene age of the Mogollón Formation also implies the co-occurrence of two late and remote species of *Carodnia* (i.e., *C. vieirai* in Itaboraian levels of southeastern Brazil and *C. inexpectans* in Itaboraian or Riochican deposits of coastal northern Peru). It also confirms the persistence of the order Xenungulata well after the Paleocene-Eocene transition, as considered by Gelfo et al. (2009) and Woodburne et al. (2014a, 2014b). Interestingly, there is no xenungulate record attested during the Selandian and Thanetian standard ages. The apparent northward shift of the xenungulate geographical range, with early Paleocene occurrences restricted to high latitudes and early Eocene ones at mid- and low latitudes (Fig. 1b), is most probably an artifact, due to the incompleteness of the early Cenozoic fossil record at the South American scale.

Furthermore, *Carodnia* is one of the first mammalian genera to be shown having such a large cosmopolitan distribution on the South American supercontinental island (Figs. 1b and 4; van der Geer et al. 2010) during Paleogene times. While very few early Paleogene mammals of northern South America are known (e.g., Negri et al. 2010; Antoine 2012; Antoine et al. 2012; Bloch et al. 2012; Jaramillo 2012), the case of *Carodnia* questions the probable absence of significant paleogeographic barriers – at least for large land mammals – across South America in the concerned interval and further suggests the existence of ubiquitous taxa in the corresponding realm. At a lower taxonomic scale, the divergence between the varied *Carodnia* species may however have been guided by regional events, such as early Andean tectonic pulses.

**Acknowledgments** Walter Aguirre prepared the specimen for the Museo de Historia Natural de la Universidad Nacional Mayor San Marcos, in Lima. The manuscript highly benefited from discussion and debate with Maëva J. Orliac and Rodolphe Tabuce. Javier N. Gelfo, an anonymous reviewer, and John R. Wible provided very constructive remarks on earlier versions of the manuscript. The excavation was partly funded by the Institut des Sciences de l'Evolution, Montpellier. This is ISE-M Publication n° 2014–119 S.

## Appendix 1. Character list

1. *Coronoid canal*: (0) absent; (1) present. An obstructed canal is scored 1.
2. *Mandibular foramen*: (0) located below the upper edge of the dentary; (1) located above the edge of the dentary.
3. *Coronoid crest (crest of the masseteric fossa along the anterior border of the coronoid process)*: (0) absent or weakly developed; (1) transversely thick; (2) hypertrophied and laterally flaring with a very deep masseteric fossa posterior to it. Modified from character 21 of Luo and Wible (2005).
4. *Mandibular ramus, anterior edge*: (0) posterior to m3; (1) partly hiding m3 in lateral view.
5. *Mandibular ramus*: (0) pointing anterodorsally; (1) vertical; (2) pointing posterodorsally.
6. *Mandibular body*: (0) low with respect to m3 length; (1) high as in *Carodnia inexpectans* sp. nov.; (2) very high, as in *C. vieirai*. Additive states.
7. *Mandibular body, facial vein notch*: (0) absent; (1) present.
8. *Lower molars*: (0) equal size for m1-m3; (1) m1 much smaller than m2-3.
9. *Ratio between occlusal areas of m3/m2*: (0) >1.5; (1) comprised between 1.0 and 1.5; (2) <1.0. Additive states.
10. *Precingulid on m2-m3*: (0) strongly developed; (1) weak.
11. *Precingular stylid on m2 and m3*: (0) absent; (1) present.
12. *Paraconid on m2-3*: (0) present; (1) absent. Modified from characters 1 and 2 of Gelfo et al. (2008: Table 1). Reversed states.
13. *Paraconid on m2-3*: (0) twinned with the metaconid; (1) well separated from the metaconid. Modified from characters 1 and 2 of Gelfo et al. (2008: Table 1).
14. *Trigonid on m2-3*: (0) with paracristid distally concave in occlusal view and closing the trigonid; (1) with paracristid long, low and almost parallel to the protolophid. Simplified from characters 3 and 4 of Gelfo et al. (2008: Table 1).
15. *Distal wall of the trigonid on m2-m3*: (0) 'V'-shaped protocristid, with well differentiated protoconid and metaconid; (1) protolophid well developed, high, and with wear facet projected distally well differentiated. Simplified from characters 7 and 8 of Gelfo et al. (2008: Table 1). Reversed states.
16. *Hypoconid on m2*: (0) well individualized and bunoid; (1) as part of a lophid with cristid obliqua and hypoconulid; (2) as part of the hypolophid (sensu Gelfo et al. 2008). Character 11 of Gelfo et al. (2008).
17. *Hypoconid on m3*: (0) well individualized and bunoid; (1) as part of a lophid with cristid obliqua and hypoconulid; (2) as part of the hypolophid. Character 12 of Gelfo et al. (2008).
18. *Cristid obliqua on m2-m3*: (0) present; (1) absent (not differentiated from the hypolophid). Modified from characters 13 and 14 of Gelfo et al. (2008).
19. *Cristid obliqua on m2*: (0) well differentiated from the hypoconid and long; (1) as part of a lophid with the hypoconid and hypoconulid, and pointing to the medial side of the protolophid. Simplified from character 13 of Gelfo et al. (2008).
20. *Cristid obliqua on m3*: (0) well differentiated from the hypoconid and long; (1) as part of a lophid with the hypoconid and hypoconulid, and pointing to the medial side of the protolophid; (2) not lophoid, very short, and reduced. Simplified from character 14 of Gelfo et al. (2008).
21. *Entoconid on m2*: (0) bunoid and well differentiated; (1) transverse forming an entolophid; (2) undifferentiated from the hypolophid; (3) associated to the hypoconulid as a lophid that joins the postcristid and entocristid. Character 19 of Gelfo et al. (2008).
22. *Entoconid on m3*: (0) bunoid and well differentiated; (1) associated to the hypoconulid as a lophid that joins the postcristid and entocristid. Simplified from character 20 of Gelfo et al. (2008).
23. *Hypoconulid on m2*: (0) not differentiated from a lophid that also joins the entoconid; (1) as part of the hypolophid. Simplified from character 15 of Gelfo et al. (2008).
24. *Hypoconulid on m2*: (0) well differentiated from other talonid cusps/lophids; (1) not differentiated or as part of other talonid cusps/lophids. Simplified from character 15 of Gelfo et al. (2008).
25. *Talonid/protolophid widths on m3*: (0) equal; (1) narrower; (2) much narrower. Additive states.
26. *Relative position of entoconid/hypoconid on m3*: (0) more distal; (1) almost at the same level.
27. *Paracristid on m3*: (0) strongly developed; (1) weak.
28. *Premetacristid on m3*: (0) strong; (1) smooth.
29. *Protolophid on m3*: (0) oblique; (1) transverse.
30. *Ectocingulid on m3*: (0) faint or absent; (1) thick and continuous.
31. *Talonid on m3*: (0) low with respect to the trigonid in lateral view; (1) as high as the trigonid.
32. *Hypoconulid on m3*: (0) high; (1) low.
33. *Ectocingulid on the talonid of m3*: (0) absent; (1) present.
34. *Posterior root on m3*: (0) vertical; (1) pointing distoventrally.

**Appendix 2. Taxon-character matrix used for the phylogenetic analysis. Character numbers are bold-typed. See Appendix 1 for further detail on character states**

<i>Taxa</i>	0000000001 <b>1111111112</b> 2222222223 3333
	1234567890 1234567890 1234567890 1234
<i>Alcidedorbignya inopinata</i>	0020101110 0010011011 1010100100 0000
<i>Asmithwoodwardia scotti</i>	0010200010 0010000011 0000000000 100?
<i>Didolodus multicuspis</i>	?0?0?0?010 0000000000 00-00?00-0 100?
<i>Notoetayoaa gargantuaia</i>	1??0?1???0 10101?0??2 ?1??200?00 1101
<i>Etayoaa bacatensis</i>	?020?21100 1010110012 3110100110 0001
<i>Carodnia feruglioii</i>	?????????1 11-11201-- 2111101100 0111
<i>Carodnia cf. feruglioii</i>	??21????111 11-1120??- 2111101101 0?0?
<i>Carodnia vieirai</i>	1121021111 01-11201-- 2111101101 0111
<i>Carodnia inexpectans</i> sp. nov.	1121011120 11-11201-- 2111111110 0001

## References

- Ameghino F (1897) Mammifères crétacés de l'Argentine: Deuxième Contribution à la connaissance de la Faune Mammalogique des Couches à *Pyrotherium*. Bol Inst Geogr Argent 18:406–521
- Antoine PO (2002) Phylogénie et évolution des Elasmotheriina (Mammalia, Rhinocerotidae). Mém Mus Natl Hist Nat 188:1–359
- Antoine PO (2012) Cenozoic mammals from Amazonia: diversity, environment, and biogeography. J Vertebr Paleontol 32(Suppl to 3):57
- Antoine PO, Marivaux L, Croft DA, Billet G, Ganerød M, Jaramillo C, Martin T, Orliac MJ, Tejada J, Duranthon F, Fanjat G, Rousse S, Salas-Gismondi R (2012) Middle Eocene rodents from Peruvian Amazonia reveal the pattern and timing of caviomorph origins and biogeography. Proc Roy Soc B 279:1319–1326
- Bayona G, Montenegro O, Cardona A, Jaramillo C, Lamus F, Morón S, Quiroz L, Ruiz MC, Valencia V, Parra M., Stockli D (2010) Estratigrafía, procedencia, subsidencia y exhumación de las unidades Paleógenas en el Sinclinal de Usme, sur de la zona axial de la Cordillera Oriental. Geol Colomb 35:5–35
- Bergqvist LP (1996) Reassociação do pós-crâneo às espécies de ungulados da bacia de S. J. de Itaboráí (Paleoceno), Estado do Rio de Janeiro, e filogenia dos “Condylarthra” e ungulados sul-americanos com base no pós-crâneo. PhD Dissertation, Universidade Federal do Rio Grande do Sul, Brazil
- Bergqvist LP, Powell JE, Avilla LS (2004) A new xenungulate from the Río Loro Formation (Paleocene) from Tucumán province (Argentina). Ameghiniana Suppl 41:36R
- Bloch JJ, Rincón AF, Head JJ, Herrera F, Jaramillo CA (2012) Early Eocene mammals from the hot tropics of northern South America. J Vertebr Paleontol 32(Suppl to 3):64
- Bremer K (1994) Branch support and tree stability. Cladistics 10:295–304
- Cifelli RL (1993) The phylogeny of the native South American ungulates. In: Szalay FS, Novacek MJ, McKenna MC (eds) Mammal Phylogeny, Volume 2: Placentals. Springer Verlag, New York, pp 195–216
- Clyde WC, Wilf P, Iglesias A, Slingerland RL, Barnum T, Bijl PK, Bralower TJ, Brinkhuis H, Comer EE, Huber BT, Ibañez-Mejia M, Jicha BR, Krause JM, Schueth JD, Singer BS, Raigemborn MS, Schmitz MD, Sluijs A, Zamalloa M del C (2014) New age constraints for the Salamanca Formation and lower Río Chico Group in the western San Jorge Basin, Patagonia, Argentina: implications for K/Pg extinction recovery and land mammal age correlations. Geol Soc Am Bull 126:289–306
- Damuth J (1990) Problems in estimating body masses of archaic ungulates using dental measurements. In: Damuth J, MacFadden BJ (eds) Body Size in Mammalian Paleobiology: Estimation and Biological Implications. Cambridge University Press, Cambridge, pp 229–253
- Farris JS (1988) Hennig86 reference, version 1.5. Port Jefferson Station (software and manual)
- Ferretti MP, Debruyne R (2011) Anatomy and phylogenetic value of the mandibular and coronoid canals and their associated foramina in proboscideans (Mammalia). Zool J Linn Soc 161:391–413
- Fildani A (2004) Analysis of two arc-associated basins and onset of their deep-water stages: Magallanes basin, Chile, and Talara Basin, Peru. PhD Dissertation, Stanford University, Palo Alto, California
- Fildani A, Hessler AM, Graham SA (2008) Trench-forearc interactions reflected in the sedimentary fill of Talara basin, northwest Peru. Basin Research 20:305–331.
- Gelfo JN (2010) The “condylarth” Didolodontidae from Gran Barranca: history of the bunodont South American mammals up to the Eocene–Oligocene transition. In: Madden RH, Carlini AA,

- Vucetich MG, Kay RF (eds) The Paleontology of Gran Barranca. Evolution and Environmental Change through the Middle Cenozoic of Patagonia. Cambridge University Press, Cambridge, pp 130–142
- Gelfo JN, López GM, Bond M (2008) A new Xenungulata (Mammalia) from the Paleocene of Patagonia, Argentina. *J Paleontol* 82:329–335
- Gelfo JN, Goin FJ, Woodburne MO, Muizon C de (2009) Biochronological relationships of the earliest South American Paleogene mammalian faunas. *Palaeontology* 52:251–269
- Higley D (2004) The Talara Basin province of northwestern Peru: Cretaceous-Tertiary total petroleum system, US Geol Surv Bull 2206-A
- Hoorn C, Wesselingh FP, ter Steege H, Bermudez MA, Mora A, Sevink J, Sammartin I, Sanchez-Meseguer A, Anderson CL, Figueiredo JP, Jaramillo C, Riff D, Negri FR, Hooghiemstra H, Lundberg J, Stadler T, Sarkinen T, Antonelli A (2010) Amazonia through time: Andean uplift, climate change, landscape evolution, and biodiversity. *Science* 330:927–931
- Iddings A, Olsson AA (1928) Geology of northwest Perú. *Bull Am Assoc Petrog Geol* 12:1–39
- Jaramillo CA (2012) Fossil vertebrates from Neotropical latitudes: a vast record waiting to be discovered. *J Vertebr Paleontol* 32(Suppl to 3):116
- Legendre S (1989) Les communautés de mammifères du Paléogène (Eocène supérieur et Oligocène) d'Europe occidentale: structures, milieux et évolution. *Münch geowiss Abh* 16:1–110
- Line SRP, Bergqvist LP (2005) Enamel structure of Paleocene mammals of the São José de Itaboráí basin, Brazil. 'Condylartha', Litopterna, Notoungulata, Xenungulata, and Astrapotheria. *J Vertebr Paleontol* 25:924–928
- Louterbach M, Roddaz M, Bailleul J, Antoine PO, Adnet S, Kim JH, van Soelen E, Parra F, Gérard J, Calderon Y, Gagnaison C, Sinninghe Damsté JS, Baby P (2014) Evidences for a late Palaeocene marine incursion in southern Amazonia (Madre de Dios Sub-Andean Zone, Peru). *Palaeogeogr Palaeoclimatol Palaeoecol*. doi:[10.1016/j.palaeo.2014.09.027](https://doi.org/10.1016/j.palaeo.2014.09.027)
- Lundberg JG, Marshall LG, Guerrero J (1998) The stage of Neotropical fish diversification: a history of tropical South American rivers. In: Malabarba LR, Reis RE, Vari RP, Lucena ZM, Lucena CAS (eds). Phylogeny and classification of neotropical fishes. Edipucrs, Porto Alegre, pp 13–48
- Luo ZX, Wible JR (2005) A Late Jurassic digging mammal and early mammalian diversification. *Science* 308:103–107
- Morón S, Fox DL, Feinberg JM, Jaramillo C, Bayona G, Montes C, Bloch JI (2013) Climate change during the early Paleogene in the Bogotá Basin (Colombia) inferred from paleosol carbon isotope stratigraphy, major oxides, and environmental magnetism. *Palaeogeogr Palaeoclimatol Palaeoecol* 388:115–127
- Muizon C de, Marshall LG (1987) Le plus ancien Pantodonte (Mammalia), du Crétacé supérieur de Bolivie. *CR Acad Sci Paris* 304:205–208
- Muizon C de, Marshall LG (1992) *Alcidedorbignya inopinata* (Mammalia: Pantodonta) from the early Paleocene of Bolivia; phylogenetic and paleobiogeographic implications. *J Paleontol* 66:499–520
- Negri FR, Bocquentin Villanueva J, Ferigolo J, Antoine PO (2010) A review of Tertiary mammal faunas and birds from western Amazonia. In: Hoorn C, Wesselingh FP (eds). Amazonia, landscape and species evolution: A look into the past. Blackwell-Wiley, Oxford, pp 245–258
- O'Leary MA, Bloch JI, Flynn JJ, Gaudin TJ, Giallombardo A, Giannini NP, Goldberg SL, Kraatz BP, Zhe-Xi Luo, Jin Meng, Xijun Ni, Novacek MJ, Perini FA, Randall ZS, Rougier GW, Sargis EJ, Silcox MT, Simmons NB, Spaulding M, Velasco PM, Weksler M, Wible JR, Cirranello AL (2013) The placental mammal ancestor and the post-K-Pg radiation of placentals. *Science* 339:662–667
- Paula Couto C (1952) Fossil mammals from the beginning of the Cenozoic in Brazil: Condylathra, Litopterna, Xenungulata, and Astrapotheria. *Bull Am Mus Nat Hist* 99:355–394
- Petters V (1968) Stratigraphic Memorandum No. 13: The Basal Salina Formation. Unpubl report, International Petroleum Corporation of Peru
- Roddaz M, Hermoza W, Mora A, Baby P, Parra M, Christophoul F, Brusset S, Espurt N (2010) Cenozoic sedimentary evolution of the Amazonian foreland basin system, In: Hoorn C, Wesselingh FP (eds) Amazonia, Landscape and Species Evolution: A Look into the Past. Blackwell-Wiley, Oxford, pp 61–88
- Séranne M (1987) Evolution tectono-sédimentaire du Bassin de Talara (nord-ouest du Pérou). *Bull Inst Fr Et And* 16:103–125
- Shockley BJ, Anaya F (2004) *Pyrotherium macfaddeni*, sp. nov. (late Oligocene, Bolivia) and the pedal morphology of pyrotheres. *J Vertebr Paleontol* 24:481–488
- Simpson GG (1935) Descriptions of the oldest known South American mammals, from the Rio Chico Formation. *Am Mus Novitates* 93:1–25
- Swofford DL (1998) PAUP, Phylogenetic Analysis Using Parsimony, version 4.0, Smithsonian Institution, Sinauer Associates, Sunderland, Massachusetts (software)
- Tabuce R, Jaeger JJ, Marivaux L, Salem M, Bilal AA, Benammi M, Chaimanee Y, Coster P, Marandat B, Valentín X, Brunet M (2012) New stem elephant-shrews (Mammalia, Macroscelidea) from the Eocene of Dur At-Talah, Libya. *Palaeontology* 55:945–955
- Tassy P, Shoshani J (1988) The Thethytheria: elephants and their relatives. In: Benton MJ (ed) The Phylogeny and Classification of Tetrapods. II. Mammals. Clarendon Press, Oxford, pp 283–315
- van der Geer A, Lytras G, de Vos J, Dermitzakis M (2010) Front Matter. In: van der Geer A, Lytras G, de Vos J, Dermitzakis M (eds) Evolution of Island Mammals: Adaptation and Extinction of Placental Mammals on Islands. Wiley-Blackwell, Oxford. doi:[10.1002/9781444323986.fmatter](https://doi.org/10.1002/9781444323986.fmatter)
- Villarroel C (1987) Características y afinidades de *Etayoia* n. gen., tipo de una nueva familia de xenungulata (Mammalia) del Paleoceno medio de Colombia. *Com Paleontol Mus Montevideo* 19:241–253
- Wilson LA, Sánchez-Villagra MR, Madden RH, Kay RF (2012) Testing a developmental model in the fossil record: molar proportions in South American ungulates. *Paleobiology* 38:308–321
- Woodburne MO, Goin FJ, Bond M, Carlini AA, Gelfo JN, López GM, Iglesias A, Zimicz AN (2014a) Paleogene land mammal faunas of South America; a response to global climatic changes and indigenous floral diversity. *J Mammal Evol* 21:1–73
- Woodburne MO, Goin FJ, Raigemborn MS, Heizler M, Gelfo JN, Oliveira EV (2014b) Revised timing of the South American early Paleogene land mammal ages. *J S Am Earth Sci* 54:109–119
- Zachos JC, Dickens GR, Zeebe RE (2008) An early Cenozoic perspective on greenhouse warming and carbon-cycle dynamics. *Nature* 451: 279–283